Received: 21 October 2016 | Revised: 20 November 2016 | Accepted: 10 December 2016

DOI 10.1002/aoc.3735

FULL PAPER

WILEY Applied Organometallic Chemistry

Effect of lipophilicity of wingtip groups on the anticancer potential of mono N-heterocyclic carbene silver(I) complexes: Synthesis, crystal structures and *in vitro* anticancer study

Tabinda Fatima[1] | Rosenani A. Haque[1] | Mohd R. Razali[1] | Ashfaq Ahmad[2] | Muhammad Asif[3] | Mohamed B. Khadeer Ahamed[4] | A. M. S. Abdul Majid[3]

[1] School of Chemical Sciences, Universiti Sains Malaysia, 11800 USM, Penang, Malaysia

[2] School of Pharmaceutical Sciences, Universiti Sains Malaysia, 11800 USM, Penang, Malaysia

[3] EMAN Research and Testing Laboratory School of Pharmacy, Universiti Sains Malaysia, 11800 USM, Penang, Malaysia

[4] EMAN Biodiscoveries Sdn. Bhd., Suite 126, Level 1, EUREKA Complex, Universiti Sains Malaysia (USM), Minden 11800, Penang, Malaysia

Correspondence
Rosenani A. Haque, School of Chemical Sciences, Universiti Sains Malaysia, 11800 USM, Penang, Malaysia.
Email: rosenani@usm.my

Funding information
Research University Individual Grant, Grant/Award Number: RUI/1001/PKIMIA/811346

A series of symmetrically *n*-alkyl-substituted mono benzimidazolium salts with steady increase in *n*-alkyl chain length have been prepared by stepwise *N*-alkylation resulting in salts (**1**–**8**). The mono N-heterocyclic carbene (NHC)–Ag(I) complexes (**9**–**16**) derived from the respective salts were readily accessible by *in situ* deprotonation using Ag_2O. All the salts and the complexes were characterized using Fourier transform infrared, ^{1}H NMR, ^{13}C NMR and elemental analyses. Furthermore, the structures of salts **3** and **7** and complex **16** were elucidated using X-ray crystallography, which established that this mono NHC–Ag(I) complex has a linear bis-carbene arrangement (C_2–Ag). The proligands and the respective Ag(I) complexes were studied for their *in vitro* anticancer potential against human colon cancer cell line (HCT-116) using 5-fluorouracil as a standard. From the IC_{50} values of all the tested compounds, it can be postulated that there is an influential relationship between the increase in chain length of the wingtip *n*-alkyl groups and the anticancer potential. The proligands **4**–**8** and their respective complexes **12**–**16** with long *n*-alkyl chain lengths (n = 6–10) showed better IC_{50} values (0.3–3.9 μM) than the standard drug with the complexes displaying markedly better antiproliferation activity against HCT-116 cell line than the respective proligands and the standard drug (IC_{50} = 10.2 μM).

KEYWORDS
benzimidazolium salts, human colon cancer cell line (HCT-116), N-heterocyclic–Ag(I) complexes

1 | INTRODUCTION

Carbenes are strong electrophiles in a free state and become strong nucleophiles when present in an N-heterocyclic system. N-heterocyclic carbenes (NHCs) are a well-known class of ligands with the ability to form complexes with almost all main group metals[1] as well as transition metals[2–4] including the rare earth metals.[5–7] Ag(I) complexes of NHCs are much focused upon among the NHC metal complexes regarding their synthesis and diverse applications. Apart from their widespread use in transmetallation[8,9] and catalysis,[10,11] Ag(I)–NHC complexes are gaining importance in the biological field where they are studied for their antibacterial properties and are of great interest in terms of anticancer activity.[12–14]

Mono- and bis-imidazolium and benzimidazolium-derived Ag(I)–NHC complexes, with functionalized and non-functionalized substituents, have been studied for their anticancer potential by various research groups[14–18] including ours,[19–22] where the Ag(I)–NHC complexes have been

tested against a variety of cancer cell lines and are found to have some promising anticancer activities. In one study of the mechanism of cancer cell death by Ag(I)–NHC complexes, it was reported that these complexes induce depolarization of the mitochondrial membrane potential, allowing the release of mitochondrial proteins and causing early apoptosis[23] and thereby proving them as potential chemotherapeutic agents.

In the reported cytotoxicity studies addressing the effect of a steady increase in chain length across the mono-imidazolium salts, it was found that cytotoxicity increases with an increase in the alkyl chain length.[24] The bis-benzimidazolium salts, on the other hand, are reported to have lower cytotoxicity with longer alkyl chains, whereas the corresponding Ag(I)–NHC complexes are found to manifest significant activity with an increase in alkyl chain length.[25] To the best of our knowledge, there are no reported data on the effect of an increase in chain length of the wingtip *n*-alkyl groups across the mono-benzimidazolium salts and their respective mono NHC–Ag(I) complexes.

In the work presented here, the anticancer potential of a series of synthesized mono Ag(I)–NHC complexes and their respective proligands was studied. The inspiration for this study comes from the fact that the parent benzimidazole moiety and the incorporated Ag(I) both have their individual biological significance.[26–28] The purpose of introducing the alkyl chain substituents is twofold: firstly, the substituent does not have its own activity when reaching the target; secondly, it acts as an excipient that helps the Ag(I)–NHC complex to pass through the lipophilic cell membrane and enter the cell where it can produce its anticancer effect.

2 | EXPERIMENTAL

2.1 | Materials and instrumentation

All the chemicals and solvents were of analytical grade and were used as received. Furier transform infrared (FT-IR) spectra were recorded with a PerkinElmer 2000 spectrometer. ^{1}H NMR and ^{13}C NMR spectral analyses were conducted with a Bruker 500 MHz spectrometer. Elemental analysis was conducted with a PerkinElmer series II 2400 microanalyser. Melting points were obtained using a Stuart Scientific SMP-1 (UK) instrument.

2.2 | Synthesis of *N*-alkylbenzimidazoles

N-Alkylbenzimidazoles were readily accessible in good yields by reacting benzimidazole and *n*-alkyl bromide (n = 3–10) following a reported literature procedure.[29]

2.3 | Synthesis of *N*,*N*-*n*-alkylbenzimidazolium bromide

2.3.1 | Synthesis of *N*,*N*-*n*-propylbenzimidazolium bromide (1)

To a solution of *N*-*n*-propylbenzimidazole (1.00 g, 5.00 mmol) in 30 ml of dioxane, propyl bromide (0.61 g, 5.00 mmol) was added with stirring and was refluxed at 110 °C for 24 h. On cooling to room temperature the *N*,*N*-*n*-propylbenzimidazolium bromide salt appeared as an oily layer, the solvent was decanted and the salt was left to crystallize at room temperature in a fume cupboard. The salt was collected as a colourless crystalline material. Yield 1.06 g (71%); m.p. 121–125 °C. Anal. Calcd for $C_{13}H_{19}BrN_2{\cdot}H_2O$ (%): C, 51.84; H, 6.97; N, 9.30. Found (%): C, 51.75; H, 7.10; N, 9.32. FT-IR (KBr, ν, cm^{-1}): 3132, 3044 (C_{arom}—H), 2934, 2855 (C_{aliph}—H), 1610, 1462, 1427 (C_{arom}=C_{arom}), 1561 (C_{arom}—N), 1290 (C_{aliph}—N). ^{1}H NMR (500 MHz, DMSO-d_6, δ, ppm): 0.92 (6H, 2 × CH_3, t, J = 7.5 Hz), 1.94–1.99 (4H, 2 × —CH_2—, m), 4.52 (4H, 2 × —CH_2—, t, J = 7.0 Hz), 7.42–7.49 (2H, Ar-H, m), 7.81–7.88 (2H, Ar-H, m), 10.01 (1H, NCHN, s). ^{13}C NMR (125 MHz, DMSO-d_6, δ, ppm): 10.7 (CH_3); 11.2, 23.4, 46.4 (CH_2); 111.5, 112.1, 118.7, 123.9, 133.3 (Ar-C); 142.1 (NCHN).

2.3.2 | Synthesis of *N*,*N*-*n*-butylbenzimidazolium bromide (2)

The procedure was similar to that for compound **1**, but using *N*-*n*-butylbenzimidazole (0.87 g, 5.00 mmol) instead of *N*-*n*-propylbenzimidazole. Salt **2** was collected as a colourless crystalline solid. Yield 1.20 g (77%); m.p. 132–136 °C. Anal. Calcd for $C_{15}H_{23}BrN_2{\cdot}H_2O$ (%): C, 54.72; H, 7.60; N, 8.51. Found (%): C, 54.70; H, 7.95; N, 8.43. FT-IR (KBr, ν, cm^{-1}): 3125, 3033 (C_{arom}—H), 2931, 2870 (C_{aliph}—H), 1615, 1461, 1430 (C_{arom}=C_{arom}), 1563 (C_{arom}—N), 1209 (C_{aliph}—N). ^{1}H NMR (500 MHz, DMSO-d_6, δ, ppm): 0.93 (6H, 2 × CH_3, t, J = 7.5 Hz), 1.31–1.39 (4H, 2 × —CH_2—, m), 1.89–1.94 (4H, 2 × —CH_2—, m), 4.51 (4H, 2 × —CH_2—N, t, J = 7.0 Hz), 7.66–7.72 (2H, Ar-H, m), 8.10–8.13 (2H, Ar-H, m), 9.89 (1H, NCHN, s). ^{13}C NMR (125 MHz, DMSO-d_6, δ, ppm): 13.4 (CH_3); 19.1, 46.4 (CH_2); 113.7, 126.5, 131.1 (Ar-C); 142.1 (NCHN).

2.3.3 | Synthesis of *N*,*N*-*n*-pentylbenzimidazolium bromide (3)

The procedure was similar to that for compound **1**, but using *N*-*n*-pentylbenzimidazole (1.00 g, 5.50 mmol) instead of *N*-*n*-propylbenzimidazole. Salt **3** was collected as a colourless crystalline solid. Yield 1.45 g (77%); m.p. 122–126 °C. Anal. Calcd for $C_{17}H_{27}BrN_2{\cdot}H_2O$ (%): C, 57.15; H, 8.12; N, 7.84.

Found (%): C, 57.07; H, 8.21; N, 7.83. FT-IR (KBr, ν, cm^{-1}): 3124, 3037 (C_{arom}—H), 2954, 2859 (C_{aliph}—H), 1614, 1465, 1427 (C_{arom}=C_{arom}), 1568 (C_{arom}—N), 1263 (C_{aliph}—N). ^{1}H NMR (500 MHz, DMSO-d_6, δ, ppm): 0.87 (6H, 2 × CH_3, t, J = 7.0 Hz), 1.29–1.34 (8H, 4 × —CH_2—, m), 1.89–1.96 (4H, 2 × —CH_2—, m), 4.51 (4H, 2 × —CH_2—N, t, J = 7.0 Hz), 7.69–7.72 (2H, Ar-H, m), 8.10–8.14 (2H, Ar-H, m), 9.92 (1H, NCHN, s). ^{13}C NMR (125 MHz, DMSO-d_6, δ, ppm): 13.7 (CH_3); 21.5, 27.8, 28.1, 46.6 (CH_2); 113.7, 126.5, 131.1 (Ar-C); 142.1 (NCHN).

2.3.4 | Synthesis of *N*,*N*-*n*-hexylbenzimidazolium bromide (4)

The procedure was similar to that for compound **1**, but using *N*-*n*-hexylbenzimidazole (1.00 g, 5.00 mmol) instead of *N*-*n*-propylbenzimidazole. Salt **4** was collected as a colourless crystalline solid. Yield 1.30 g (71%); m.p. 113–117 °C. Anal. Calcd for $C_{19}H_{31}BrN_2{\cdot}H_2O$ (%): C, 59.23; H, 8.57; N, 7.27. Found (%): C, 59.19; H, 8.78; N, 7.21. FT-IR (KBr, ν, cm^{-1}): 3118, 3038 (C_{arom}—H), 2954, 2843 (C_{aliph}—H), 1609, 1483, 1449 (C_{arom}=C_{arom}), 1556 (C_{arom}—N), 1293 (C_{aliph}—N). ^{1}H NMR (500 MHz, DMSO-d_6, δ, ppm): 0.85 (6H, 2 × CH_3, t, J = 7.0 Hz), 1.25–1.33 (12H, 6 × —CH_2—, m), 1.89–1.94 (4H, 2 × —CH_2—, m), 4.51 (4H, 2 × —CH_2—N, t, J = 7.0 Hz), 7.69–7.72 (2H, Ar-H, m), 8.10–8.14 (2H, Ar-H, m), 9.92 (1H, NCHN, s). ^{13}C NMR (125 MHz, DMSO-d_6, δ, ppm): 13.8 (CH_3); 21.7, 25.4, 28.4, 30.6, 46.6 (CH_2); 113.7, 126.5, 131.1 (Ar-C), 142.1 (NCHN).

2.3.5 | Synthesis of *N*,*N*-*n*-heptylbenzimidazolium bromide (5)

The procedure was similar to that for compound **1**, but using *N*-*n*-heptylbenzimidazole (1.00 g, 4.50 mmol) instead of *N*-*n*-propylbenzimidazole. Salt **5** was collected as a colourless crystalline solid. Yield 1.30 g (73%); m.p. 101–105 °C. Anal. Calcd for $C_{21}H_{35}BrN_2{\cdot}H_2O$ (%): C, 61.03; H, 8.96; N, 6.78. Found (%): C, 61.21; H, 9.21; N, 6.77. FT-IR (KBr, ν, cm^{-1}): 3113, 3025 (C_{arom}—H), 2926, 2850 (C_{aliph}—H), 1609, 1466, 1424 (C_{arom}=C_{arom}), 1557 (C_{arom}—N), 1283 (C_{aliph}—N). ^{1}H NMR (500 MHz, DMSO-d_6, δ, ppm): 0.85 (6H, 2 × CH_3, t, J = 7.0 Hz), 1.24–1.32 (16H, 8 × —CH_2—, m), 1.89–1.95 (4H, 2 × —CH_2—, m), 4.51 (4H, 2 × —CH_2—N, t, J = 7.0 Hz), 7.69–7.72 (2H, Ar-H, m), 8.10–8.14 (2H, Ar-H, m), 9.90 (1H, NCHN, s). ^{13}C NMR (125 MHz, DMSO-d_6, δ, ppm): 13.8 (CH_3); 21.9, 25.7, 28.4, 31.0, 46.6 (CH_2); 113.7, 126.5, 131.1 (Ar-C); 142.1 (NCHN).

2.3.6 | Synthesis of *N*,*N*-*n*-octylbenzimidazolium bromide (6)

The procedure was similar to that for compound **1**, but using *N*-*n*-octylbenzimidazole (1.00 g, 4.50 mmol) instead of *N*-*n*-propylbenzimidazole. Salt **6** was collected as a colourless crystalline solid. Yield 1.60 g (84%); m.p. 110–114 °C. Anal. Calcd for $C_{23}H_{39}BrN_2{\cdot}H_2O$ (%): C, 62.59; H, 9.29; N, 6.35. Found (%): C, 62.78; H, 9.52; N, 6.42. FT-IR (KBr, ν, cm^{-1}): 3118, 3022 (C_{arom}—H), 2946, 2847 (C_{aliph}—H), 1613, 1466, 1422 (C_{arom}=C_{arom}), 1557 (C_{arom}—N), 1271 (C_{aliph}—N). ^{1}H NMR (500 MHz, DMSO-d_6, δ, ppm): 0.84 (6H, 2 × CH_3, t, J = 7.0 Hz), 1.22–1.31 (20H, 10 × —CH_2—, m), 1.89–1.92 (4H, 2 × —CH_2—, m), 4.51 (4H, 2 × —CH_2—N, t, J = 7.0 Hz), 7.69–7.72 (2H, Ar-H, m), 8.10–8.14 (2H, Ar-H, m), 9.92 (1H, NCHN, s). ^{13}C NMR (125 MHz, DMSO-d_6, δ, ppm): 13.8 (CH_3); 22.0, 25.7, 28.4, 31.1, 46.6 (CH_2-N); 113.7, 126.5, 131.1 (Ar-C); 142.0 (NCHN).

2.3.7 | Synthesis of *N*,*N*-*n*-nonylbenzimidazolium bromide (7)

The procedure was similar to that for compound **1**, but using *N*-*n*-nonylbenzimidazole (1.00 g, 4.00 mmol) instead of *N*-*n*-propylbenzimidazole. Salt **7** was collected as a colourless crystalline solid. Yield 1.30 g (72%); m.p. 106–111 °C. Anal. Calcd for $C_{25}H_{43}BrN_2{\cdot}H_2O$ (%): C, 63.97; H, 9.59; N, 5.97. Found (%): C, 64.12; H, 9.64; N, 6.18. FT-IR (KBr, ν, cm^{-1}): 3117, 3025 (C_{arom}—H), 2918, 2854 (C_{aliph}—H), 1610, 1485, 1424 (C_{arom}=C_{arom}), 1557 (C_{arom}—N), 1290 (C_{aliph}—N). ^{1}H NMR (500 MHz, DMSO-d_6, δ, ppm): 0.83 (6H, 2 × CH_3, t, J = 7.0 Hz), 1.21–1.31 (24H, 12 × —CH_2—, m), 1.90–1.93 (4H, 2 × —CH_2—, m), 4.50 (4H, 2 × —CH_2-N, t, J = 7.0 Hz), 7.70–7.72 (2H, Ar-H, m), 8.11–8.13 (2H, Ar-H, m), 9.92 (1H, NCHN, s). ^{13}C NMR (125 MHz, DMSO-d_6, δ, ppm): 13.8 (CH_3); 21.7, 25.6, 28.4, 28.9, 29.3, 31.2, 44.1, 46.6 (CH_2); 113.7, 126.5, 131.1 (Ar-C); 143.9 (NCHN).

2.3.8 | Synthesis of *N*,*N*-*n*-decylbenzimidazolium bromide (8)

The procedure was similar to that for compound **1**, but using *N*-*n*-decylbenzimidazole (1.00 g, 4.00 mmol) instead of *N*-*n*-propylbenzimidazole. Salt **8** was collected as a colourless crystalline solid. Yield 1.50 g (79%); m.p. 116–119 °C. Anal. Calcd for $C_{13}H_{19}BrN_2{\cdot}H_2O$ (%): C, 65.20; H, 9.86; N, 5.63. Found (%): C, 65.26; H, 10.08; N, 5.62. FT-IR (KBr, ν, cm^{-1}): 3118, 3026 (C_{arom}—H), 2954, 2847 (C_{aliph}—H), 1609, 1468, 1422 (C_{arom}=C_{arom}), 1556 (C_{arom}—N), 1285 (C_{aliph}—N). ^{1}H NMR (500 MHz, DMSO-d_6, δ, ppm): 0.83 (6H, 2 × CH_3, t, J = 7.0 Hz), 1.20–1.27 (28H,

14 × —CH_2—, m), 1.89–1.91 (4H, 2 × —CH_2—, m), 4.48 (4H, 2 × —CH_2—N, t, J = 7.0 Hz), 7.67–7.72 (2H, Ar-H, m), 8.10–8.12 (2H, Ar-H, m), 9.86 (1H, NCHN, s). ^{13}C NMR (125 MHz, DMSO-d_6, δ, ppm): 13.8 (CH_3); 22.1, 25.6, 28.5, 31.2, 46.6 (CH_2); 113.7, 126.5, 131.1 (Ar-C) 141.9 (NCHN).

2.4 | Synthesis of *N*,*N*-*n*-alkylbenzimidazol-2-ylidene silver(I) hexafluorophosphate

2.4.1 | Synthesis of *N*,*N*-*n*-propylbenzimidazol-2-ylidene silver(I) hexafluorophosphate (9)

The *N*,*N*-*n*-propylbenzimidazolium bromide salt (1.00 g, 3.50 mmol) was dissolved in 150 ml of methanol in a round-bottom flask wrapped with aluminium foil and silver oxide (0.80 g, 3.50 mmol) was added to it. Under exclusion of light the reaction mixture was allowed to stir for 2 days at room temperature. After completion of the reaction time the reaction mixture was filtered through a pad of celite in order to remove all the insoluble species like AgBr and any unreacted Ag_2O. To the clear solution containing the *N*,*N*-*n*-propylbenzimidazol-2-ylidene silver(I) bromide, potassium hexafluorophosphate (1.34 g, 7.28 mmol) was added and was allowed to stir for 2 h. This metathesis reaction resulted in the formation of methanol-insoluble *N*,*N*-*n*-propylbenzimidazol-2-ylidene silver(I) hexafluorophosphate which was filtered, washed with distilled water in order to remove any unreacted KPF_6 and allowed to dry in a fume cupboard. Complex **9** was obtained in the form of white powder after drying. Yield 1.50 g (50%); m.p. 182–185 °C. Anal. Calcd for $C_{26}H_{36}AgF_6N_4P{\cdot}2H_2O$ (%): C, 45.3; H, 5.77; N, 8.08. Found (%): C, 45.13; H, 5.98; N, 8.24. FT-IR (KBr, ν, cm^{-1}): 3037 (C_{arom}—H), 2968, 2877 (C_{aliph}—H), 1614, 1465, 1404 (C_{arom}=C_{arom}), 1519 (C_{arom}—N), 1145 (C_{aliph}—N). ^{1}H NMR (500 MHz, DMSO-d_6, δ, ppm): 0.92 (6H, 2 × CH_3, t, J = 7.5 Hz), 1.94–1.99 (4H, 2 × —CH_2—, m), 4.52 (4H, 2 × —CH_2—, t, J = 7.0 Hz), 7.45–7.72 (4H, Ar-H, m). ^{13}C NMR (125 MHz, DMSO-d_6, δ, ppm): 11.2 (CH_3); 23.4, 46.4 (CH_2); 111.5, 112.1, 118.7, 123.9, 133.3 (Ar-C); 187.9 (C2-Ag, br d).

2.4.2 | Synthesis of *N*,*N*-*n*-butylbenzimidazol-2-ylidene silver(I) hexafluorophosphate (10)

Complex **10** was prepared by following the same procedure as that for complex **9** except that salt **1** was replaced with salt **2** (1.00 g, 3.00 mmol), Ag_2O (0.70 g, 3.00 mmol), KPF_6 (1.10 g, 6.00 mmol). Complex **10** was obtained in the form of white powder after drying. Yield 1.50 g (70%); m.p. 119–121 °C. Anal. Calcd for $C_{30}H_{44}AgF_6N_4P$ (%): C, 50.50; H, 6.17; N, 7.85. Found (%): C, 50.16; H, 6.25; N, 7.70. FT-IR (KBr, ν, cm^{-1}): 3057 (C_{arom}—H), 2962, 2866 (C_{aliph}—H), 1607, 1481, 1411 (C_{arom}=C_{arom}), 1141 (C_{aliph}—N). ^{1}H NMR (500 MHz, DMSO-d_6, δ, ppm): 0.98 (6H, 2 × CH_3, t, J = 7.5 Hz), 1.43–1.47 (4H, 2 × —CH_2—, m), 1.97–2.01 (4H, 2 × —CH_2—, m), 4.54 (4H, 2 × —CH_2—N, t, J = 7.0 Hz), 7.49–7.52 (2H, Ar-H, m), 7.72–7.79 (2H, Ar-H, m). ^{13}C NMR (125 MHz, DMSO-d_6, δ, ppm): 12.8 (CH_3); 19.7, 32.1, 48.8 (CH_2); 111.9, 113.7, 117.1, 123.9, 126.7, 133.7 (Ar-C); 187.9 (C2-Ag, br d).

2.4.3 | Synthesis of *N*,*N*-*n*-pentylbenzimidazol-2-ylidene silver(I) hexafluorophosphate (11)

Complex **11** was prepared by following the same procedure as that for complex **9** except that salt **1** was replaced with salt **3** (1.00 g, 3.00 mmol), Ag_2O (0.70 g, 3.00 mmol), KPF_6 (1.10 g, 6.00 mmol). Complex **11** was obtained in the form of white powder after drying. Yield 1.40 g (51%); m.p. 110–114 °C. Anal. Calcd for $C_{34}H_{52}AgF_6N_4P$ (%): C, 53.06; H, 6.76; N, 7.28. Found (%): C, 52.97; H, 6.94; N, 7.45. FT-IR (KBr, ν, cm^{-1}): 3038 (C_{arom}—H), 2968, 2877 (C_{aliph}—H), 1615, 1469, 1401 (C_{arom}=C_{arom}), 1519 (C_{arom}—N), 1143 (C_{aliph}—N). ^{1}H NMR (500 MHz, DMSO-d_6, δ, ppm): 0.89 (6H, 2 × CH_3, t, J = 7.0 Hz), 1.32–1.38 (8H, 4 × —CH_2—, m), 1.93–1.99 (4H, 2 × —CH_2—, m), 4.54 (4H, 2 × —CH_2—N, t, J = 7.0 Hz), 7.47–7.50 (2H, Ar-H, m), 7.71–7.73 (2H, Ar-H, m). ^{13}C NMR (125 MHz, DMSO-d_6, δ, ppm): 12.9 (CH_3); 21.8, 27.8, 49.0 (CH_2); 111.7, 113.2, 117.1, 123.9, 133.4 (Ar-C); 187.6 (C2-Ag, br d).

2.4.4 | Synthesis of *N*,*N*-*n*-hexylbenzimidazol-2-ylidene silver(I) hexafluorophosphate (12)

Complex **12** was prepared by following the same procedure as that for complex **9** except that salt **1** was replaced with salt **4** (1.00 g, 2.70 mmol), Ag_2O (0.60 g, 2.70 mmol), KPF_6 (1.00 g, 5.50 mmol). Complex **12** was obtained in the form of white powder after drying. Yield 1.60 g (64%); m.p. 97–99 °C. Anal. Calcd for $C_{38}H_{60}AgF_6N_4P$ (%): C, 55.28; H, 7.27; N, 6.78. Found (%): C, 54.90; H, 7.47; N, 6.71. FT-IR (KBr, ν, cm^{-1}): 3076 (C_{arom}—H), 2923, 2859 (C_{aliph}—H), 1479, 1453 (C_{arom}=C_{arom}), 1191 (C_{aliph}—N). ^{1}H NMR (500 MHz, DMSO-d_6, δ, ppm): 0.84 (6H, 2 × CH_3, t, J = 7.0 Hz), 1.26–1.44 (12H, 6 × —CH_2—, m), 1.97–2.03 (4H, 2 × —CH_2—, m), 4.54 (4H, 2 × —CH_2—N, t, J = 7.0 Hz), 7.49–7.52 (2H, Ar-H, m), 7.73–7.74 (2H, Ar-H, m). ^{13}C NMR (125 MHz, DMSO-d_6, δ, ppm): 12.9 (CH_3); 21.8, 25.4, 28.8, 30.6, 49.0 (CH_2); 111.7, 113.2, 117.1, 123.9, 133.4 (Ar-C); 187.6 (C2-Ag, br d).

2.4.5 | Synthesis of *N*,*N*-*n*-heptylbenzimidazol-2-ylidene silver(I) hexafluorophosphate (13)

Complex **13** was prepared by following the same procedure as that for complex **9** except that salt **1** was replaced with salt **5** (1.00 g, 2.50 mmol), Ag_2O (0.60 g, 2.50 mmol), KPF_6 (0.90 g, 5.00 mmol). Complex **13** was obtained in the form of white powder after drying. Yield 1.50 g (62%); m.p. 90–92 °C. Anal. Calcd for $C_{42}H_{68}AgF_6N_4P$ (%): C, 57.21; H, 7.72; N, 6.36. Found (%): C, 56.87; H, 7.85; N, 6.29. FT-IR (KBr, ν, cm^{-1}): 3063 (C_{arom}—H), 2930, 2854 (C_{aliph}—H), 1477, 1454 (C_{arom}=C_{arom}), 1141 (C_{aliph}—N). ^1H NMR (500 MHz, DMSO-d_6, δ, ppm): 0.82 (6H, 2 × CH_3, t, J = 7.0 Hz), 1.20–1.44 (16H, 8 × —CH_2—, m), 1.96–2.03 (4H, 2 × —CH_2—, m), 4.54 (4H, 2 × —CH_2—N, t, J = 7.0 Hz), 7.49–7.52 (2H, Ar-H, m), 7.73–7.78 (2H, Ar-H, m). ^{13}C NMR (125 MHz, DMSO-d_6, δ, ppm): 13.0 (CH_3); 21.8, 22.1 25.9, 26.2, 28.9, 30.1, 31.1, 45.1, 49.0 (CH_2); 111.7, 113.2, 117.1, 123.6, 126.6, 133.4 (Ar-C); 187.6 (C2-Ag, br d).

2.4.6 | Synthesis of *N*,*N*-*n*-octylbenzimidazol-2-ylidene silver(I) hexafluorophosphate (14)

Complex **14** was prepared by following the same procedure as that for complex **9** except that salt **1** was replaced with salt **6** (1.00 g, 2.40 mmol), Ag_2O (0.50 g, 2.40 mmol), KPF_6 (0.90 g, 4.80 mmol). Complex **14** was obtained in the form of white powder after drying. Yield 1.20 g (50%); m.p. 87–89 °C. Anal. Calcd for $C_{46}H_{76}AgF_6N_4P$ (%): C, 58.92; H, 8.11; N, 5.98. Found (%): C, 58.68; H, 8.19; N, 5.97. FT-IR (KBr, ν, cm^{-1}): 3061 (C_{arom}—H), 2927, 2851 (C_{aliph}—H), 1479, 1407 (C_{arom}=C_{arom}), 1137 (C_{aliph}—N). ^1H NMR (500 MHz, DMSO-d_6, δ, ppm): 0.79 (6H, 2 × CH_3, t, J = 7.0 Hz), 1.19–1.25 (20H, 10 × —CH_2—, m), 1.97–2.03 (4H, 2 × —CH_2—, m), 4.54 (4H, 2 × —CH_2—N, t, J = 7.0 Hz), 7.49–7.52 (2H, Ar-H, m), 7.72–7.75 (2H, Ar-H, m). ^{13}C NMR (125 MHz, DMSO-d_6, δ, ppm): 13.0 (CH_3); 21.8, 25.7, 26.4, 28.6, 29.8, 31.2, 45.2, 48.9 (CH_2); 111.7, 113.2, 117.1, 123.9, 133.4 (Ar-C); 187.6 (C2-Ag, br d).

2.4.7 | Synthesis of *N*,*N*-*n*-nonylbenzimidazol-2-ylidene silver(I) hexafluorophosphate (15)

Complex **15** was prepared by following the same procedure as that for complex **9** except that salt **1** was replaced with salt **7** (1.00 g, 2.20 mmol), Ag_2O (0.50 g, 2.20 mmol), KPF_6 (0.80 g, 4.40 mmol). Complex **15** was obtained in the form of white powder after drying. Yield 1.40 g (62%); m.p. 94–96 °C. Anal. Calcd for $C_{50}H_{84}AgF_6N_4P$ (%): C, 60.43; H, 8.46; N, 5.64. Found (%): C, 59.98; H, 8.58; N, 5.61. FT-IR (KBr, ν, cm^{-1}): 3063 (C_{arom}—H), 2918, 2853 (C_{aliph}—H), 1481, 1450 (C_{arom}=C_{arom}), 1199 (C_{aliph}—N). ^1H NMR (500 MHz, DMSO-d_6, δ, ppm): 0.80 (6H, 2 × CH_3, t, J = 7.0 Hz), 1.18–1.23 (24H, 12 × —CH_2—, m), 1.96–2.02 (4H, 2 × —CH_2—, m), 4.54 (4H, 2 × —CH_2—N, t, J = 7.0 Hz), 7.49–7.51 (2H, Ar-H, m), 7.73–7.74 (2H, Ar-H, m). ^{13}C NMR (125 MHz, DMSO-d_6, δ, ppm): 12.9 (CH_3); 21.8, 25.6, 26.4, 28.5, 29.9, 31.2, 45.2, 48.9 (CH_2); 111.7, 113.2, 117.1, 123.8, 126.6, 133.4 (Ar-C); 187.5 (C2-Ag, br d).

2.4.8 | Synthesis of *N*,*N*-*n*-decylbenzimidazol-2-ylidene silver(I) hexafluorophosphate (16)

Complex **16** was prepared by following the same procedure as that for complex **9** except that salt **1** was replaced with salt **8** (1.00 g, 2.00 mmol), Ag_2O (0.48 g, 2.00 mmol), KPF_6 (0.70 g, 4.00 mmol). Complex **16** was obtained in the form of white powder after drying. Yield 1.10 g (55%); m.p. 99–102 °C. Anal. Calcd for $C_{54}H_{92}AgF_6N_4P$ (%): C, 61.78; H, 8.77; N, 5.34. Found (%): C, 61.37; H, 9.05; N, 5.24. FT-IR (KBr, ν, cm^{-1}): 3045 (C_{arom}—H), 2920, 2852 (C_{aliph}—H), 1469, 1401 (C_{arom}=C_{arom}), 1140 (C_{aliph}—N). ^1H NMR (500 MHz, DMSO-d_6, δ, ppm): 0.82 (6H, 2 × CH_3, t, J = 7.0 Hz), 1.17–1.21 (28H, 14 × —CH_2—, m), 1.97–2.01 (4H, 2 × —CH_2—, m), 4.53 (4H, 2 × —CH_2—N, t, J = 7.0 Hz), 7.49–7.52 (2H, Ar-H, m), 7.73–7.75 (2H, Ar-H, m). ^{13}C NMR (125 MHz, DMSO-d_6, δ, ppm): 12.9, 13.1 (CH_3); 21.8, 22.1, 26.3, 28.8, 29.8, 31.3, 48.9 (CH_2); 111.7, 113.2, 117.1, 123.9, 126.6, 133.4 (Ar-C); 187.5 (C2-Ag, br d).

2.5 | Crystallographic details

Crystals of compounds **3**, **7** and **16** were mounted on fine glass fibre using viscous hydrocarbon oil. Data were collected using a Bruker-Smart ApexII-2009 CCD diffractometer equipped with graphite monochromater and using Mo Kα (λ = 0.71073) radiation. Data collection for compound **3** was conducted at room temperature while for **7** and **16** the temperature was maintained at 100 K using open flow N_2 cryostreams. The integration was carried out with the program SAINT using the APEX^{II} software as reported.[30] Solutions were obtained by direct methods using SHELXS-2014, followed by successive refinements using full matrix least squares method against F^2 using SHELXL-2014.[31] The program X-seed was used as graphical SHELX interface.[32] The data for **3**, **7** and **16** are summarized in Table 1.

2.6 | *In vitro* anticancer studies

2.6.1 | Materials and equipment

Rosewell Park Memorial Institute (RPMI 1640) cell culture medium was obtained from ScienCell, USA. Microplate reader (Epoch, BioTek, USA), methylthiazolyldiphenyl

TABLE 1 Crystal data and structure refinement parameters for **3**, **7** and **16**

	3	7	16
Empirical formula	$C_{17}H_{29}ON_2Br$	$C_{25}H_{45}ON_2Br$	$C_{54}H_{92}ON_4Ag{\cdot}F_6P$
Formula weight	357.52	469.53	1050.16
Crystal system	Monoclinic	Triclinic	Orthorhombic
Space group	$P2_1/c$	P-1	$Pnna$
a (Å)	8.8572(8)	8.8529(3)	37.0015(11)
b (Å)	22.553(2)	9.1496(3)	12.3952(4)
c (Å)	9.9406(9)	16.8044(6)	12.2836(4)
α (°)	90	80.9102(9)	90
β (°)	105.0785(13)	77.4971(9)	90
γ (°)	90	77.7698(9)	90
V (Å^3)	1917.3(3)	1289.73(8)	5633.8(3)
Z	4	2	4
Density calcd (g cm^{-3})	1.238	1.209	1.238
μ (mm^{-1})	2.146	1.611	0.443
F(000)	752	504	2240
T (K)	297(2)	100(2)	100(2)
θ range (°)	2.01–30.01	2.3–32.9	1.7–30.9
Reflections collected	42 059	68 985	11 2448
Reflections unique	5579	9510	8829
Reflections obs [$I > 2\sigma(I)$]	2813	8522	7557
R_{int}	0.044	0.030	0.054
R_1 (obs, all)	0.0699	0.0241	0.0599
wR_2 (obs, all)	0.1907	0.0595	0.0971
Goodness of fit	1.032	1.046	1.411

tetrazolium bromide (MTT) reagent and heat-inactivated foetal bovine serum (HIFBS) were purchased from Gibco, UK. Penicillin/streptomycin solution and 5-fluorouracil (5-FU) were purchased from Sigma-Aldrich, Germany.

Other equipment was as follows: dissecting microscope (Motic, Taiwan), Eppendorf tips (AxyGEN, USA), Eppendorf tube 1.5 ml (Eppendorf, Germany), incubator (Binder Fisher Scientific, Germany), inverted fluorescent microscope (Olympus, Japan), inverted light microscope (Matrix Optic (M) Sdn. Bhd, Japan), ImageJ software (http://rsb.info.nih.gov/ij/), laminar flow (class II; ESCO-BSC, Singapore), micropipette (Eppendorf, USA), refrigerator (Samsung, Japan), serological pipette 10, 5 ml (TPP®, USA), water bath (PROTECH-Electronic, Malaysia) and 6-well cell culture plate (Coster Corning, USA).

2.6.2 | Cell lines and environmental conditions

Human colorectal tumour (HCT-116) cell line was purchased (Rockvill, MD, USA). HCT-116 cell line was kept in RPMI 1640 cell culture medium with a supply of 10% HIFBS and 10% penicillin/streptomycin solution. Temperature was maintained at 37 °C.

2.6.3 | Preparation of cell culture

The first step in the preparation is the growth of HCT-116 cell line under incubation conditions. Only those cells were selected for plating purposes which reached about 70–80% level of confluency. Medium used in the plates previously was aspirated and cells used were washed with phosphate buffer saline solution two to three times. After washing with phosphate buffer saline solution, trypsin was added evenly on the cell surfaces. Cells were incubated for 1 min at 37 °C. Cell segregation was facilitated by simply tapping the flask containing the cells and was observed under a microscope. A volume of 5 ml of fresh medium was added to inhibit trypsin activity. After counting, there was a final concentration of 2.5×10^5 cells ml^{-1} which was later inoculated to the wells of a 96-well plate (100 µl of cells per well). These seeded

plates were then incubated at standard atmospheric conditions for cell culture.

2.6.4 | MTT assay for measuring cell viability

Volumes of 100 µl of the cells were seeded in all wells of a 96-well microplate and the microplate was incubated overnight for cell attachment under CO_2 incubator. Later on, a volume of 100 µl of each test substance was added in each well and the plate was labelled accordingly. Different dilutions of the test substance were prepared to investigate any dose-dependent response. After the addition of test substance into the plate containing cancer cells, the plate was incubated at 37 °C with 5% CO_2 environment for 72 h. After 72 h of treatment, a volume of 20 µl of MTT reagent was added into each well and again incubated for 4 h. After this period of incubation, 20 µl of DMSO (MTT lysis solution) was added in each well. Plates were further incubated for 5 min under the same environment of incubation. Finally, absorbance was measured at 570 and 620 nm using a microplate reader (Epoch, BioTek, USA). Data were analysed for cell viability and percent inhibition of proliferation of test substances. The results were presented as percent viability compared to the negative control (mean ± SD, $n = 3$).[33]

3 | RESULTS AND DISCUSSION

3.1 | Synthesis

In general, the first *N*-alkylation was performed using potassium hydroxide as a base for the removal of acidic (N—H) protons in a reaction mixture of benzimidazole in DMSO and subsequent reaction with the respective *n*-alkyl bromide. The *N*-*n*-alkylbenzimidazole, after extraction with chloroform and evaporation, was then reacted with *n*-alkyl bromide in 1,4-dioxane under reflux for 24 h. The oily product was separated and left to crystallize at room temperature for 3–4 days. All the resultant symmetrically substituted *N*,*N*-*n*-alkylbenzimidazolium bromide salts were obtained in a colourless crystalline state in medium to high yield. These salts are stable towards air and moisture, are soluble in polar organic solvents such as methanol, DMSO and acetonitrile and almost insoluble in diethyl ether and petroleum ether.

For the generation of carbene and complexation with Ag(I), the *in situ* deprotonation method involving Ag_2O was used.[34] After two days of stirring of reaction mixture containing *N*-*n*-alkylbenzimidazolium bromide salt with Ag_2O (1:1 ratio) in methanol, the resulting Ag(I) complex was separated from the insoluble AgBr and any unreacted Ag_2O by filtration through celite. The obtained NHC–Ag(I) complex in bromide form was converted to hexafluorophosphate form by a metathesis reaction. This conversion was done for the purpose of easy handling and to achieve complex purity. All the *N*,*N*-*n*-alkylbenzimidazol-2-ylidene silver(I) hexafluorophosphate complexes were obtained in a powder form in good yields. These complexes are readily soluble in acetonitrile and DMSO and almost insoluble in methanol, diethyl ether and petroleum ether. The synthesis of mono benzimidazolium salts and their respective mono NHC–Ag(I) complexes is depicted in Scheme 1. The structures of salts **1**–**8** and their respective Ag(I) complexes **9**–**16** were established by a combination of ^{1}H NMR and ^{13}C NMR spectroscopy and elemental analysis. As the NMR and the FT-IR spectra of all the salts and complex **9** showed strong peak and absorption band for water, so the amount of water was estimated for the elemental analysis and the percentages of C, H and N are in good accord with their calculated values. The molecular structures of salts **3** and **7** and complex **16** were further supported by X-ray diffraction data.

3.2 | FT-IR analysis

FT-IR spectral analysis of all the *N*-*n*-alkylbenzimidazolium bromide salts and their respective Ag(I) complexes was carried out using the KBr pellet method. As the substituents are simple alkyl chains, the prominent absorptions in the functional group region are the (═C—H) stretching vibrations of medium to low intensity in the region 3000–3100 cm^{-1} and the (—C—H) aliphatic stretching vibrations of strong intensity at 2800–2900 cm^{-1}. The (C═C) stretching vibrations of aromatic ring occur as medium absorption bands in the range 1400–1600 cm^{-1}. The (C═N) stretching vibrations appear in the form of strong and sharp absorption bands between 1550 and 1600 cm^{-1} while the (C—N) stretching

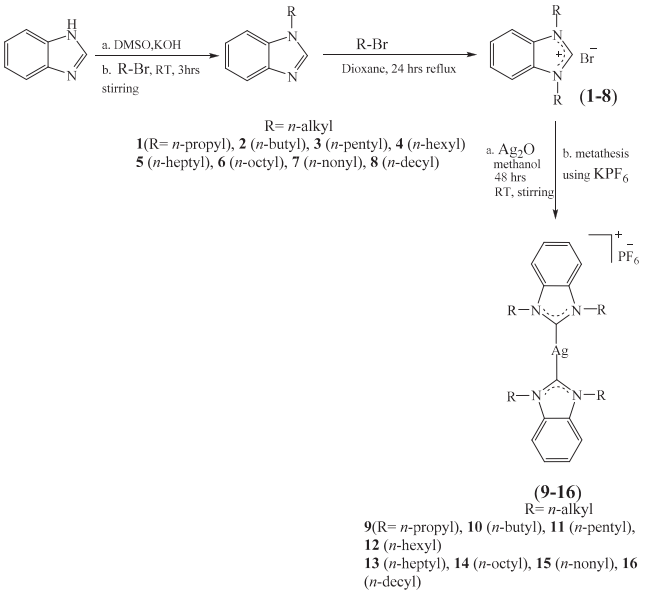

SCHEME 1 Synthesis of *N*,*N*-*n*-alkylbenzimidazolium bromide salts (**1**–**8**) and their respective *N*,*N*-*n*-alkylbenzimidazol-2-ylidene silver(I) hexafluorophosphate complexes (**9**–**16**)

vibrations give medium to weak bands in the region 1100–1200 cm^{-1}.[35] The accessible FT-IR region does not give any indication about (C─Ag) bond whose stretching vibrations appear below 400 cm^{-1} meaning that all the NHC–Ag(I) complexes exhibit almost the same absorption bands as the *N*,*N*-*n*-alkylbenzimidazolium bromide salts. The most notable change is observed in the carbene to nitrogen absorption band where the bond length increases on complexation and can be seen in the X-ray crystallographic data. This increase in the bond length results in a lower vibrational frequency of the (C_2─N) bond with a corresponding shift of its absorption band to lower frequency and consequently this band cannot be distinguished from the (C═C) stretching absorption bands of the NHC–Ag(I) complexes.

3.3 | ^{1}H NMR and ^{13}C NMR analysis

^{1}H NMR spectra of all the *N*,*N*-*n*-alkylbenzimidazolium bromide salts were obtained in DMSO-d_6 and those of the respective complexes in acetonitrile-d_3. The resonances of all the alkyl chain protons with their expected multiplicities are clearly observed in the spectra of all salts. The methyl protons give a triplet in the most upfield region around 0.8–0.9 ppm, while the methylene protons exhibit a number of multiplets in the region 1–2 ppm. A clear triplet in the deshielded region around 4.5 ppm is observed which can be ascribed to the most deshielded methylene protons bonded with nitrogen of the benzimidazolium ring (N─CH_2─). The aromatic ring proton resonances are observed in the form of multiplets in the range 7.5–8.5 ppm. The most distinctive resonance in the most deshielded region around 9.8–9.9 ppm, which appears in the form of a singlet, is assigned to the most deshielded acidic proton (NC*H*N) of the benzimidazolium ring. On reaction with Ag_2O, all the salts undergo the removal of the acidic proton thereby resulting in the generation of carbene that coordinates with Ag(I).

Subsequently, on the conversion of the salts to Ag(I) complexes, the most notable change in the ^{1}H NMR spectra is the disappearance of the resonance around 9.8–9.9 ppm, signifying the formation of carbene.[36,37] In the ^{13}C NMR spectra of the salts, the most characteristic resonance that appears around 141–144 ppm is attributed to the C2 carbon (N*C*HN) which is the most deshielded carbon, in accordance with the literature.[38,39] Upon deprotonation and coordination with Ag(I), there is a shift of the C2 resonance to the more downfield region at 187–188 ppm in the form of apparent doublets as previously reported for NHC–Ag(I) complexes.[40,41] However, these doublets cannot be resolved further to study the coupling of carbene to ^{107}Ag and ^{109}Ag. Similar behaviour is observed for all the complexes of the series. The resonances of the other aromatic carbons appear between 111 and 133 ppm whereas the methyl and methylene protons have resonances in the region 12–48 ppm.

3.4 | X-ray crystallographic analysis

Salts **3** and **7** crystallize in a monoclinic system with space groups *P*-$2_1/c$ and *P*-1, respectively. The asymmetric unit for both salts consists of a symmetrically substituted benzimidazolium cation, one bromide ion and a water molecule in the lattice (Figure 1). In the crystal structures of both salts, the *n*-alkyl chains project perpendicular to the plane of the benzimidazole ring. The nitrogen to the carbene carbon bond distance ranges from 1.321(5) to 1.337(12) Å and the internal ring angle at the carbene centre (N─C─N) ranges from 111.6(3)° to 110.41(8)° (Table 2). The observed bond lengths and bond angles are well within the range of reported benzimidazolium salts.[42] In both structures, hydrogen bonds are observed in which the water molecule in the lattice behaves as hydrogen bond donor to the bromide ion.

Single crystals of complex **16** were obtained by the room temperature slow evaporation of a saturated solution of the complex in acetonitrile. Complex **16** crystallizes in an orthorhombic system with space group *Pnna*. The complex comprises one Ag(I) ion coordinating with two carbenes of the two benzimidazol-2-ylidene units; this cation is balanced by

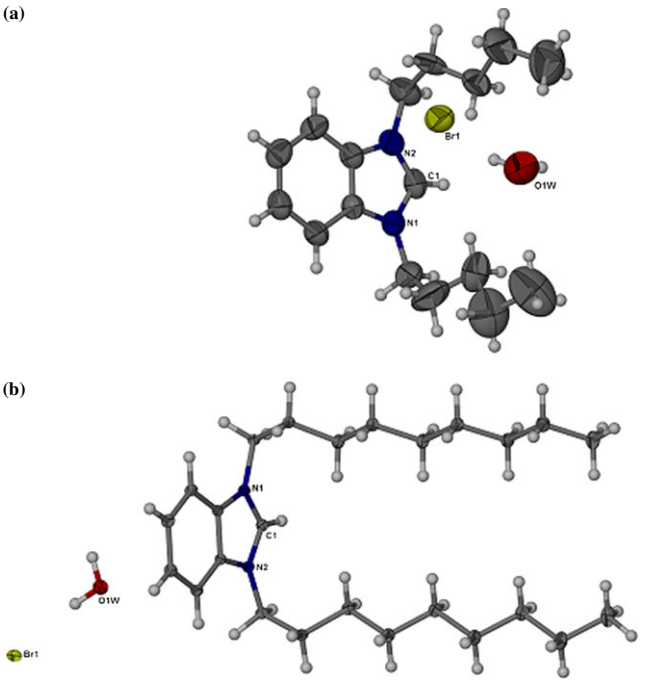

FIGURE 1 Structures of (a) **3** and (b) **7** with ellipsoids shown at 50% probability

TABLE 2 Selected bond lengths (Å) and angles (°) for salts **3** and **7**

	3	7
N1–C1/C7	1.321(5)	1.337(12)
N2–C1/C7	1.315(5)	1.334(12)
N1–C1/C7–N2	111.6(3)	110.41(8)

one hexafluorophosphate anion (Figure 2a). The resulting mono NHC–Ag(I) complex has a bis-carbene (C_2—Ag) arrangement. The two benzimidazolyl rings are almost coplanar with the *n*-decyl chains projecting perpendicular to the plane of the ring. The C1—Ag1—C1b bond has an angle of 177.10(10)° which is almost linear with the Ag1—C1 bond length of 2.088(2) Å (Table 3), this bond angle and bond distance being comparable to those found in known NHC–Ag(I) complexes.[43,44] The internal ring angle at N1—C1—N2 is 105.79(19)° with the N1—C1 bond having a bond length of 1.363(3) Å that is shorter than the N1—C2 bond with a bond length of 1.390(3) Å since this bond has more electron density due to electron-donating mesomeric effect of the nitrogens. In the three-dimensional network of complex **16** the molecules are stacked together by π–π interactions as well as non-covalent carbon chain interactions (Figure 2b).

3.5 | *In Vitro* anticancer activities of mono NHC–Ag(I) complexes and their respective proligands against HCT-116 cell line

A series of mono NHC proligands (**1**–**8**) and their corresponding complexes (**9**–**16**) were synthesized with a periodic increase in carbon chain length as wingtip groups and their anticancer activities were examined against a human colon cancer cell line. In the initial screening, all the synthesized proligands and their complexes were screened for IC_{50} values. The IC_{50} values of proligands **1**–**8** range within 1.8–31.8 μM (Table 4). These values show that an increase in the carbon chain length of the proligands causes a reduction in the IC_{50} value. It is further observed that the proligands **1**–**3** with short carbon chains have higher IC_{50} values (lower cytotoxicity). Increasing the length of the carbon chain (n = 6–10) on the proligands (**4**–**8**) results in a marked drop in the IC_{50} values (1.8–7.5) and a corresponding increase in cytotoxicity when compared to standard drug 5-FU (IC_{50} = 10.2 μμ). These observed enhanced cytotoxic effects of the proligands on human colon cancer cells validate previous findings that NHC ligands show cytotoxic effects.[18]

With the incorporation of Ag(I) ions in complexes **9**–**12** a similar trend in the cytotoxicity, as in proligands, is observed. However, increasing the carbon chain length in complexes **12**–**16** results in a greater reduction in IC_{50} values that fall within the range 0.02–3.9 μM (Table 4). These reduced IC_{50} values and the respective increased cytotoxicity can be attributed to the presence of Ag(I) ions in the complexes and an increase in carbon chain length of the wingtip groups. The increased carbon chain length enhances lipophilicity and might be the reason for the improved cytotoxicity. This present finding of an increase in carbon chain that might have facilitated the absorption of proligands and the complexes by increasing the lipophilicity is coherent with a previous study in this regard.[45] The phenomenon of increased cytotoxicity of NHC–Ag(I) complexes, in comparison to the respective proligands, is in line with previously reported data.[46]

Cancer cells have the ability to proliferate at an abnormally high rate and the present study subjected the synthesized proligands and their respective complexes to the inhibition of human colon cancer cell proliferation. The proligands **4**–**8** and complexes **12**–**16** show strong cytotoxicity against the proliferation of colorectal cancer cells (Figure 3b–f). Interestingly, the complexes exhibit improved antiproliferative

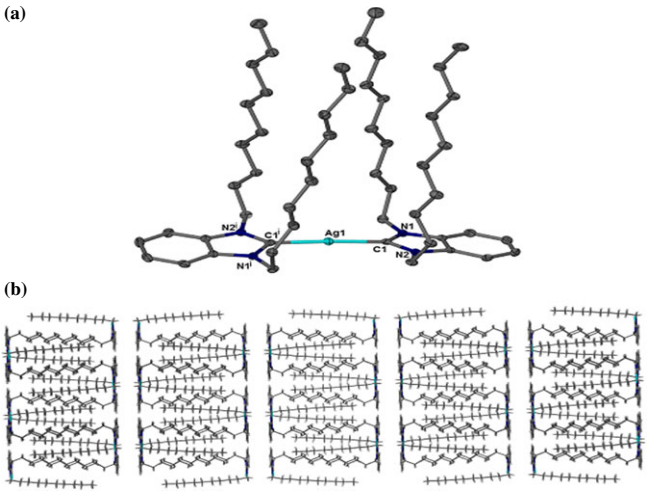

FIGURE 2 (a) Structure of **16** with ellipsoids shown at 50% probability. Hydrogen atoms and PF_6 in the lattice are omitted for clarity. (b) Packing diagram of complex **16** showing the non-covalent carbon chain interactions

TABLE 3 Selected bond lengths (Å) and angles (°) for complex **16**

Ag1–C1	2.088(2)
N1–C1	1.363(3)
N1–C2	1.390(3)
C1–Ag1–C1b	177.10(10)
N1–C1–N2	105.79(19)

TABLE 4 IC_{50} values of proligands/salts **1**–**8** and respective NHC–Ag(I) complexes **9**–**16**

Proligand	IC_{50} (μM)[a]	NHC–Ag(I) complex	IC_{50} (μM)[a]
1	31.8 ± 3.84	**9**	26.8 ± 2.30
2	27.3 ± 0.63	**10**	25.7 ± 1.27
3	30.2 ± 8.9	**11**	13.2 ± 1.50
4	7.5 ± 2.22	**12**	3.9 ± 0.62
5	3.1 ± 0.23	**13**	1.1 ± 0.28
6	2.9 ± 0.13	**14**	0.4 ± 0.05
7	1.4 ± 0.15	**15**	0.02 ± 0.02
8	1.8 ± 0.18	**16**	0.3 ± 0.12

[a]IC_{50} on HCT-116 for 5-FU = 10.2 ± 2.18 μM.

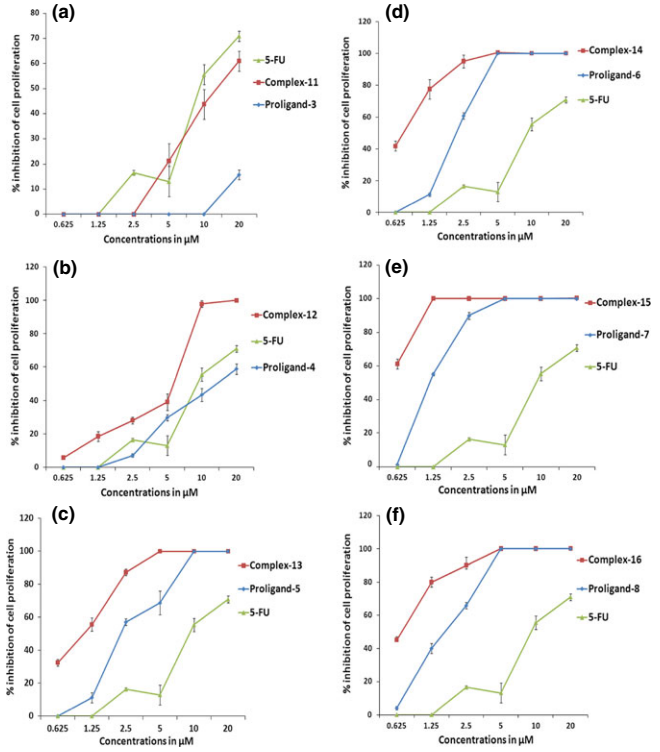

FIGURE 3 Dose-dependent antiproliferative effects of proligands **3**–**8** and complexes **11**–**16** in comparison with standard drug 5-FU. The graphs show percentage inhibition of HCT-116 cell proliferation versus concentration of test samples

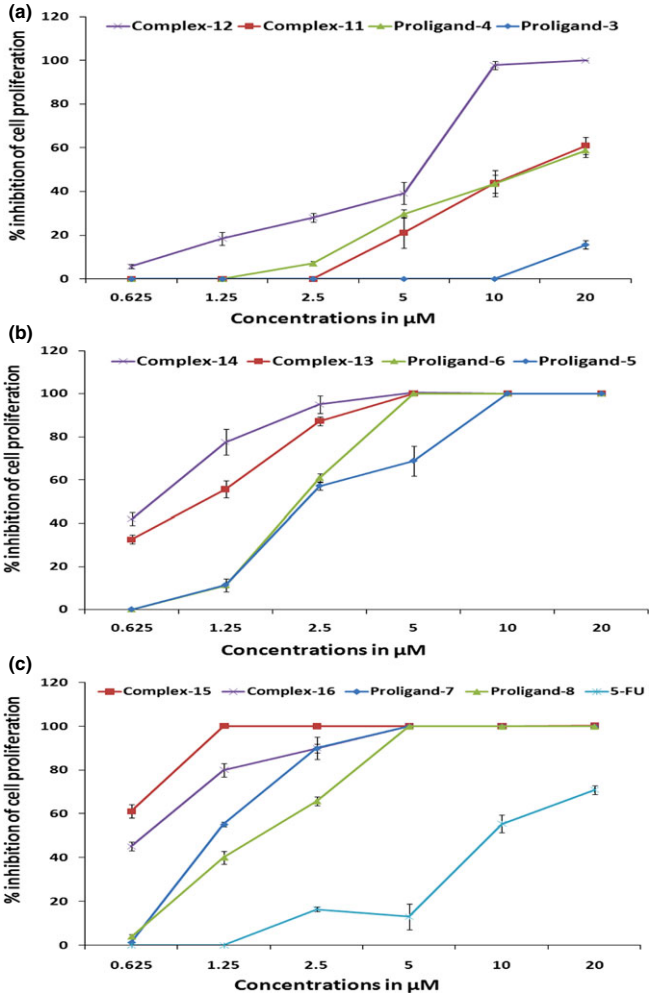

FIGURE 4 Overall mean of percentage inhibition of proliferation of active compounds against human colon carcinoma cell line in comparison with standard drug 5-FU

effects compared to the respective ligands. Moreover, it is of great significance to observe that all the proligands show better inhibition of proliferation at lowest doses when compared to the standard drug 5-FU as shown in Figure 3(b)–(f). On the other hand, proligands **1**–**3** and complexes **9** and **10** show inhibition of proliferation of cancer cells as negative values (Figure 4) and higher IC values (Table 4). However, complex **11** displays statistically significant inhibitory effect on cellular proliferation at its higher concentration (Figure 3a).

This feature of proligands **4**–**8** and their respective complexes **12**–**16** can be attributed to a variation in chain length that is reported to enhance the lipophilicity.[19] As lipids are one of the major constituents of cell and mitochondrial membranes,[47] it is assumed that the increased lipophilicity of the complexes increases the bioavailability of the Ag(I) ions into cells where they can produce cytotoxicity by inhibiting cellular respiration and causing loss of adenosine triphosphate.[48] This observation is in line with the understanding that delivery method, solubility and ionization of silver sources are important in dealing with biological systems[49] since the activity of Ag(I) ions depends on their bioavailability.[50] The proligands **4**–**8**, although having carbon chain length similar to that of their respective complexes **12**–**16**, exhibit less antiproliferative effects. A comparison between the proligands and their respective complexes against the proliferation of colon cancer cells is depicted in Figure 5. The higher antiproliferative activity of the complexes may be attributed to the presence of Ag(I) in the complex and vice versa related to the reduced antiproliferative activity of the proligands. Our findings support the previously reported data establishing the wide range of applications of NHC–Ag(I) complexes for their antibacterial to anticancer activities,[51–53] and the present study is in accordance with the data reporting metal–NHC complexes as being potent anticancer agents.[14,54]

The observed phenomenon of the effect of an increase in the chain length of the wingtip *n*-alkyl groups across the mono benzimidazolium salts and their respective mono NHC–Ag(I) complexes is depicted in Figure 4. It can be clearly seen that the proligands and the complexes with small alkyl chain length are ineffective against the proliferation of cells. However, the efficacy of the proligands and the complexes is increased with increasing chain length.

Morphological studies of the treated cells reveal potential cytotoxic changes in the cellular structures. The photomicrographic images (Figure 6) of human colon cancer cells show

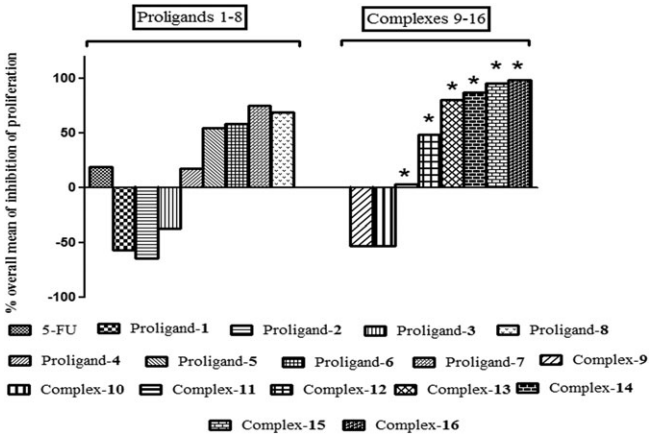

FIGURE 5 Differential inhibitory effect of proligands and complexes on proliferation of human colorectal carcinoma cell line. (A) Proligands **3** and **4** with their complexes **11** and **12** demonstrate mild cytotoxic dose-dependent response against the proliferation of HCT-116 cells. (B) Proligands **5** and **6** with their complexes **13** and **14** demonstrate moderate cytotoxic dose-dependent response against the proliferation of HCT-116 cells. (C) Proligands **7** and **8** with their complexes **15** and **16** demonstrate strong cytotoxic dose-dependent response against the proliferation of HCT-116 cells

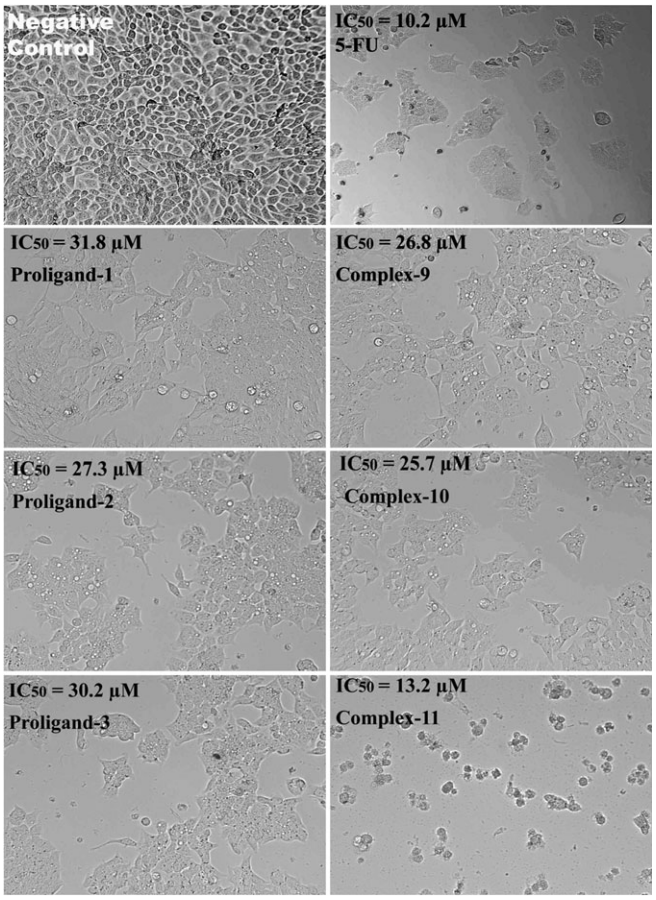

FIGURE 6 Images of human colorectal cells showing the effects of proligands **1**–**3** and complexes **9**–**11** (cell images taken under an inverted phase-contrast microscope at ×200 magnification with digital camera)

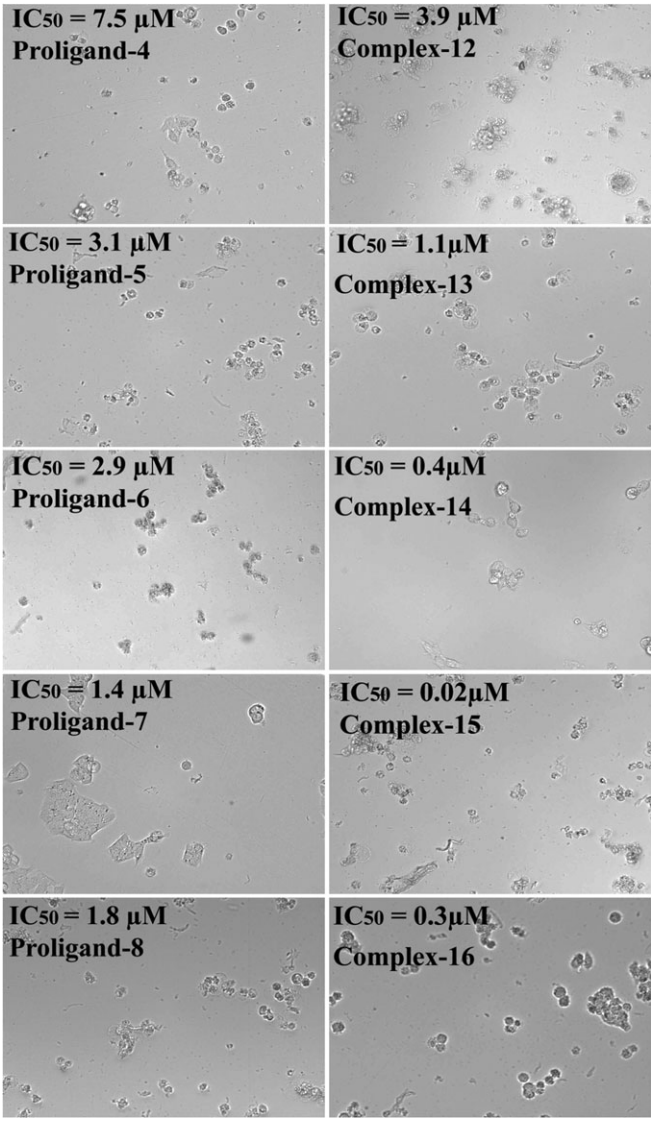

FIGURE 7 Images of human colorectal cells showing the effects of proligands **4**–**8** and complexes **12**–**16** (cell images taken under an inverted phase-contrast microscope at ×200 magnification with digital camera)

a significant shrinkage of the cells, membrane blebbing and apoptotic bodies in the cells caused by complexes **12**–**16**, whereas a moderate cytotoxic effect is observed in the cells treated with complexes **9**–**11**, since the cellular morphology is more or less similar to that of the cells from the negative control group. Complexes **12**–**16** display a more pronounced antiproliferative effect than the standard drug 5-FU (Figure 7).

4 | CONCLUSIONS

A series of mono benzimidazolium salts and their respective mono NHC–Ag(I) complexes with wingtip *n*-alkyl groups were successfully synthesized and characterized using spectral and elemental analyses. The structures of the salts and

their respective complexes were elucidated by X-ray crystallography that established a bis-carbene arrangement around the silver centre. The *in vitro* anticancer studies of the synthesized compounds against the HCT-116 cancer cell line revealed a linear relationship between an increase in the chain length of the substituents and anticancer activity. The compounds having longer *n*-alkyl chains (n = 6–10) displayed pronounced lower IC_{50} values and antiproliferative activity, with the complexes exhibiting activity many times superior to that of the proligands and standard drug 5-FU.

ACKNOWLEDGMENTS

This work was supported by Research University Individual Grant RUI/1001/PKIMIA/811346. T.F. thanks USM Fellowship (Teaching) (APEX (1002/JHEA/ATSG4001) for sponsorship.

REFERENCES

[1] D. Bourissou, O. Guerret, F. P. Gabbai, G. Bertrand, *Chem. Rev.* **2000**, *100*, 39.

[2] A. J. Arduengo III, H. V. R. Dias, J. C. Calabrese, F. Davidson, *Organometallics* **1993**, *12*, 3405.

[3] A. J. Arduengo III, S. F. Gamper, J. C. Calabrese, F. Davidson, *J. Am. Chem. Soc.* **1994**, *116*, 4391.

[4] W. A. Herrmann, K. Ofele, M. Elison, F. E. Kuhn, P. W. Roesky, *J. Org. Chem.* **1994**, *480*, c7.

[5] A. J. Arduengo III, M. Tamm, S. J. McLain, J. C. Calabrese, F. Davidson, W. J. Marshall, *J. Am. Chem. Soc.* **1994**, *116*, 7927.

[6] W. A. Herrmann, F. C. Munck, G. R. J. Artus, O. Runte, R. Anwander, *Organometallics* **1997**, *16*, 682.

[7] K. Lv, D. Cui, *Organometallics* **2008**, *27*, 5438.

[8] T. Fahlbusch, M. Frank, G. Maas, J. R. Schatz, *Organometallics* **2009**, *28*, 6183.

[9] H. J. Huang, W. C. Lee, G. P. A. Yap, T. G. Ong, *J. Org. Chem.* **2014**, *76*, 64.

[10] J. Ramirez, R. Corberan, M. Sanau, E. Peris, E. Fernandez, *Chem. Commun.* **2005**, 3056.

[11] R. Corberan, J. Ramirez, M. Poyatos, E. Peris, E. Fernandez, *Tetrahedron Asymm.* **2006**, *17*, 1759.

[12] S. Budagumpi, R. A. Haque, S. Endud, G. U. Rehman, A. W. Salman, *Eur. J. Inorg. Chem.* **2013**, 4367.

[13] W. Liu, R. Gust, *Chem. Soc. Rev.* **2013**, *42*, 755.

[14] M.-L. Teyssot, A.-S. Jarrousse, M. Manin, A. Chevry, S. Roche, F. Norre, C. Beaudoin, L. Morel, D. Boyer, R. Machiou, A. Gautier, *Dalton Trans.* **2009**, 6894.

[15] D. A. Medvetz, K. M. Hindi, M. J. Panzner, A. J. Ditto, Y. H. Yun, W. J. Youngs, *Met.-Based Drugs* **2008**, *2008*, 384010.

[16] T. J. Siciliano, M. C. Deblock, K. M. Hindi, S. Dirmus, M. J. Panzner, C. A. Tessier, W. J. Youngs, *J. Org. Chem.* **2011**, *696*, 1066.

[17] S. Patil, A. Deally, B. Gleeson, H. Muller-Bunz, F. Paradisi, M. Tacke, *Metallomics* **2011**, *3*, 74.

[18] D. C. F. Monteiro, R. M. Phillips, B. D. Crossley, J. Fielden, C. E. Willans, *Dalton Trans.* **2012**, *41*, 3720.

[19] M. A. Iqbal, R. A. Haque, S. Budagumpi, M. B. K. Ahamed, A. M. S. A. Majid, *Inorg. Chem. Commun.* **2013**, *28*, 64.

[20] R. A. Haque, M. A. Iqbal, S. Budagumpi, M. B. K. Ahamed, A. M. S. A. Majid, N. Hasanudin, *App. Organometal. Chem.* **2013**, *27*, 214.

[21] R. A. Haque, M. A. Iqbal, P. Asekunowo, M. B. K. Ahamed, A. M. S. A. Majid, M. I. Umar, *Med. Chem. Res.* **2013**, *22*, 4663.

[22] R. A. Haque, S. Y. Choo, S. Budagumpi, A. A. A. Abdullah, *Eur. J. Med. Chem.* **2015**, *90*, 82.

[23] L. Eloy, A. S. Jarrousse, M. L. Teyssot, A. Gautier, L. Morel, C. Jolivalt, *Chem. Med. Chem.* **2012**, *7*, 805.

[24] J. Ranke, K. Molter, F. Stock, U. Bottin-Weber, J. Poczobutt, J. Hoffmann, *Ecotoxicol. Environ. Saf.* **2004**, *58*, 396.

[25] M. A. Iqbal, R. A. Haque, M. B. K. Ahamed, A. M. S. A. Majid, S. S. Al-Rawi, *Med. Chem. Res.* **2013**, *22*, 2455.

[26] B. D. Narasimhan, D. Sharma, P. Kumar, *Med. Chem. Res.* **2012**, *21*, 269.

[27] A. D. Russell, W. B. Hugo, *Prog. Med. Chem.* **1994**, *31*, 351.

[28] A. Kascatan-Nebioglu, M. J. Panzner, C. A. Tessier, C. L. Cannon, W. J. Youngs, *Coord. Chem. Rev.* **2007**, *251*, 884.

[29] O. V. Starikova, G. V. Dilgushin, L. I. Larina, P. E. Ushakov, T. N. Komarova, V. A. Lopyrev, *Russian J. Org. Chem.* **2003**, 39,1467.

[30] H. Eshtiagh-Hosseini, Z. Yousefi, M. Shafiee, M. Mirzaei, *J. Coord. Chem.* **2010**, *63*, 3187.

[31] G. M. Sheldrick, *Acta Crystallogr.* **2008**, *64*, 112.

[32] L. J. Barbour, *J. Supramol. Chem.* **2001**, *1*, 189.

[33] A. F. A. Aisha, K. M. Abu-Salah, Z. Ismail, A. M. S. A. Majid, *BMC Complement. Altern. Med.* **2012**, *12*, 104.

[34] H. M. J. Wang, I. J. B. Lin, *Organometallics* **1998**, *17*, 972.

[35] M. Hranjec, K. Starcevic, S. K. Pavelic, P. Lucin, K. Pavelic, G. K. Zamola, *Eur. J. Med. Chem.* **2011**, *46*, 2274.

[36] P. O. Asekunowo, R. A. Haque, *J. Coord. Chem.* **2014**, *67*, 3649.

[37] S. Patil, K. Dietrich, A. Deally, B. Gleeson, H. Muller Bunz, F. Paradisi, *Helv. Chim. Acta* **2010**, *12*, 2347.

[38] R. A. Haque, M. A. Iqbal, P. Asekunowo, M. B. K. Ahamed, A. M. S. A. Majid, M. I. Umar, *Med. Chem. Res.* **2013**, *22*, 4663.

[39] B. Yigit, Y. Gok, I. Ozdemir, S. Gunal, *J. Coord. Chem.* **2012**, *65*, 371.

[40] I. Ozdemir, S. Demir, S. Gunal, I. Ozdemir, C. Arici, D. Ulku, *Inorg. Chim. Acta* **2010**, *363*, 3803.

[41] A. R. Knapp, M. J. Panzer, D. A. Medvetz, B. D. Wright, C. A. Tessier, W. J. Youngs, *Inorg. Chim. Acta* **2010**, *364*, 125.

[42] R. A. Haque, M. A. Iqbal, H. K. Fun, S. Arshad, *Acta Crystallogr.* **2012**, *68*, 0924.

[43] P. O. Asekunowo, R. A. Haque, M. R. Razali, *Transition Met. Chem.* **2015**, *40*, 79.

[44] R. A. Haque, U. F. M. Haziz, A. A. A. Abdullah, N. Shaheeda, M. R. Razali, *Polyhedron* **2016**, *109*, 208.

[45] S. N. Riduan, Y. Zhang, *Chem. Soc. Rev.* **2013**, *42*, 9055.

[46] M. A. Iqbal, R. A. Haque, S. F. Nasri, A. Majid, M. B. K. Ahamed, *Chem. Cent. J.* **2013**, *7*, 27.

[47] L. C. Schenkel, M. Bakovic, *Int. J. Cell Biol.* **2014**, *2014*, 709828.

[48] E. Hidalgo, C. Domínguez, *Toxicol. Lett.* **1998**, *98*, 169.

[49] A. Kascatan-Nebioglu, M. J. Panzner, C. A. Tessier, C. L. Cannon, W. J. Youngs, *Coord. Chem. Rev.* **2007**, *251*, 884.

[50] S. Silver, *FEMS Microbiol. Rev.* **2003**, *27*, 341.

[51] K. M. Hindi, M. J. Panzer, C. A. Tessier, C. L. Cannon, W. J. Youngs, *Chem. Rev.* **2009**, *109*, 3859.

[52] V. Gandin, M. Pellei, M. Marinelli, C. Marzano, A. Dolmella, M. Giorgetti, *J. Inorg. Biochem.* **2013**, *129*, 135.

[53] S. Budagumpi, R. A. Haque, S. Endud, G. U. Rehman, A. W. Salman, *Eur. J. Inorg. Chem.* **2013**, 4367.

[54] A. Gautier, F. Cisnetti, *Metallomics* **2012**, *4*, 23.

SUPPORTING INFORMATION

Additional Supporting Information may be found online in the supporting information tab for this article.

How to cite this article: Fatima T, Haque RA, Razali MR, et al. Effect of lipophilicity of wingtip groups on the anticancer potential of mono N-heterocyclic carbene silver(I) complexes: Synthesis, crystal structures and *in vitro* anticancer study. *Appl Organometal Chem*. 2017;e3735. https://doi.org/10.1002/aoc.3735